WIRELESS COMMUNICATIONS AND MOBILE COMPUTING
Wirel. Commun. Mob. Comput. (2012)
Published online in Wiley Online Library (wileyonlinelibrary.com). DOI: 10.1002/wcm.1241

RESEARCH ARTICLE

Optimal sensor and path selection for target tracking in wireless sensor networks

Majdi Mansouri[1,2]*

[1] ICD/LM2S, University of Technology of Troyes, Troyes, France
[2] College of Engineering, Electrical and Computer Engineering, Texas A & M University, Qatar

ABSTRACT

This paper addresses target tracking in wireless sensor networks where the nonlinear observed system is assumed to progress according to a probabilistic state space model. Thus, we propose to improve the use of the quantized variational filtering by jointly selecting the optimal candidate sensor that participates in target localization and its best communication path to the cluster head. In the current work, firstly, we select the optimal sensor in order to provide the required data of the target and to balance the energy dissipation in the wireless sensor networks. This selection is also based on the local cluster node density and their transmission power. Secondly, we select the best communication path that achieves the highest signal-to-noise ratio at the cluster head; then, we estimate the target position using quantized variational filtering algorithm. The best communication path is designed to reduce the communication cost, which leads to a significant reduction of energy consumption and an accurate target tracking. The optimal sensor selection is based on mutual information maximization under energy constraints, which is computed by using the target position predictive distribution provided by the quantized variational filtering algorithm. The simulation results show that the proposed method outperforms the quantized variational filtering under sensing range constraint, binary variational filtering, and the centralized quantized particle filtering. Copyright © 2012 John Wiley & Sons, Ltd.

KEYWORDS

wireless sensor networks; quantized variational filtering; best sensors selection; communication path; multi-criteria function; target tracking

***Correspondence**

Majdi Mansouri, ICD/LM2S, University of Technology of Troyes, Troyes, France.
E-mail: majdi.mansouri@utt.fr

1. INTRODUCTION

Wireless sensor network (WSN) [1] nodes are powered by small batteries, which are in practical situations non-rechargeable, either because of cost limitations or because they are deployed in hostile environments with high temperature, high pollution levels, or high nuclear radiation levels. These considerations enhance energy-saving and energy-efficient WSN designs. One approach to prolong battery lifetime is to use an efficiency criterion for sensor selection and to choose the best communication path between the candidate sensor and the cluster head (CH). In a typical WSN, sensors are employed to achieve some specific task, for example, tracking objects. These nodes are severely constrained in energy and in most cases cannot be recharged. To this goal, minimizing the communication costs between sensor nodes is critical to prolong the lifetime of sensor networks. Another important metric of sensor networks is the accuracy of the sensing result of the target in that several sensors in the same cluster can provide redundant data. Because of physical characteristics such as distance, modality, or noise model of individual sensors, data from different sensors can have various qualities. Therefore, the accuracy depends on which sensor and which communication link the CH selects.

In this paper, we investigate the problem of target tracking using a WSN composed of quantized proximity sensors. Target tracking using quantized observations is a nonlinear estimation problem that can be solved using, for example, unscented Kalman filter [2] or particle filtering (PF) [3]. Recently, a variational filtering (VF) has been proposed in [4], for solving the target tracking problem because of the following: (i) it respects the communication constraints of the sensor; (ii) the online update of the filtering distribution and its compression are simultaneously performed; and (iii) it has the nice

property of being model free, ensuring the robustness of data processing.

The VF approach was only extended to a binary sensor network considering a cluster-based scheme [5]. The binary sensor network is based on the binary proximity observation model; it consists of making a binary decision according to the strength of the perceived signal. Hence, only 1 bit is transmitted for further processing if a target is detected. At each sampling instant, only one cluster of sensors is activated according to the prediction made by the VF algorithm. Resource consumption is thus restricted to the activated cluster, where intra-cluster communications are dramatically reduced. Thanks to its power efficiency, the cluster-based scheme is also considered in this paper. As only a part of information is exploited (hard binary decision), tracking in binary sensor networks suffers from poor estimation performances.

In the current work, we are interested in cluster activation that participates in data aggregation for estimating the target position, and we assumed that the sensor node locations are known. The localization of sensor nodes is a preliminary step that should be implemented in any tracking system. Many self-localization methods have been proposed in literature such as in [6–10].

The rest of the paper is organized as follows. We first discuss related work and motivate the need for our proposed scheme in Section 2. Section 3 presents the observation model, general state evolution model, and the quantized VF (QVF) algorithm. Section 6 is devoted to the developed technique aimed at adaptively selecting the optimal candidate sensor that participates in target localization. Then, the best communication path selection scheme is presented in Section 5. Section 6 gives some numerical results. Finally, Section 7 concludes the paper.

2. RELATED WORK

Several works have been proposed in the areas of routing and sensor selection for wireless sensor networks. Some of these works have been used to maintain a regular operation (e.g., tracking) of sensor nodes even when some nodes have been compromised.

There has already been a certain amount of research in the area of sensor selection for wireless sensor networks. The work in [11] has investigated mechanisms for selecting sensors for target tracking. Selection are made on the basis of the conditional entropy of the posterior target position distribution. In [12,13], joint sensor selection and rate allocation schemes are developed. The authors in [14] proposed a centralized algorithm that uses correlated measurements by selecting the most informative sensor. Complexity results for families of utility functions are presented in [15]. The idea of using information theory in sensor management was first proposed in [16]. Sensor selection based on expected information gain was introduced for decentralized sensing systems in [17]. The mutual information (MI) between the current target position distribution and the predicted sensor observation was proposed to evaluate the expected information gain about the target position attributable to a candidate sensor in [18,19]. On the other hand, without using information theory, Yao *et al.* [20] found that the tracking accuracy depends on not only the accuracy of sensors but also their locations relative to the target position during the execution of tracking algorithms. Most of these previous work do not take into account a trade-off between the quality of sensed data, the node density, the transmitting power between one sensor and the CH, and the power stored in nodes to select the candidate sensor. They have simplified or ignored the communication costs through a sensors–CH path.

The techniques developed in [21] and [22] to activate the next most informative sensor node are based on entropy and information utility, respectively. The problem is that if the optimal path is always chosen, the nodes along the path will deplete energy more quickly than others, which greatly affects the network lifetime [23], whereas the work in [24] proposed that sometimes sub-optimal paths should be chosen depending on the probabilities to elongate the whole network lifetime. On the other hand, the accuracy of target status cannot be guaranteed, and it adds latency and computation load by tracing back the path to store the average cost. Qun Li *et al.* [25] have proposed to partition the networks into regions and computing the energy level, which may increase the overhead and lead to the degradation of the performance of the tracking accuracy.

Regarding the routing area, several contributions have been proposed in the literature. The authors in [26] proposed a minimum-cost path-routing algorithm that consists in maximizing the network lifetime. The work in [27] introduced an information-directed routing scheme that aims at maximizing the information gain. Sung *et al.* [28] have considered the routing problem for the detection of a correlated random signal field and proposed a Chernoff routing metric based on the Chernoff information.

In [29], the authors proposed a direct diffusion protocol to combine the data packets coming from different sources by eliminating redundancy and minimizing the number of transmissions. In this protocol, sensor nodes measure events and create gradients of information in their respective neighborhoods. A base station (BS) requests data by broadcasting special messages (diffused in hop-by-hop mode and broadcasted by each node to its neighbors), which describe the task to be achieved by nodes. However, this protocol may generate some extra overhead at sensor nodes. Thus, it may not be convenient to some applications (e.g., environmental monitoring) that require a continuous data delivery to BS. In order to overcome this problem, a rumor routing protocol is proposed in [30] by routing queries to only the nodes that observe a particular event rather than sending them to all nodes and flooding the entire WSN.

In [21], the authors proposed two routing techniques, namely, constrained anisotropic diffusion routing (CADR)

and information-driven sensor querying. These techniques aim to query sensors and route data in a WSN such that the latency and bandwidth are minimized whereas the information gain is maximized. On the basis of some criteria, constrained anisotropic diffusion routing diffuses queries to choose which nodes can get the data. Each node routes data based on a local information/cost gradient and application needs. Nevertheless, these techniques do not explicitly describe how the query and data are routed between sensors and BS.

The authors in [31] proposed a hierarchical clustering protocol, named TEEN, which gathers sensors into clusters with each led by a CH. The sensor nodes within a cluster send their sensed information to their CH. The CH sends aggregated data to a higher-level CH until the data reach the sink. One advantage of this protocol is its suitability for time-critical sensing applications. However, for sensing applications where periodic reports are required, TEEN is not a convenient solution because users may not get any data at all if some fixed threshold is not reached.

Du and Lin have proposed a CH relay routing protocol [32], which uses two kinds of sensors to form a heterogeneous network with a single sink: a small number of powerful high-end sensors, denoted by H-sensors, and a large number of low-end sensors, denoted by L-sensors. Both kinds of nodes are static and aware of their positions using some location service. In CH relay, a WSN is portioned into clusters, each being composed of L-sensors and led by an H-sensor. The L-sensors are responsible for sensing the environment and forwarding data packets, whereas the H-sensors take the task of data fusion within their own CH and forward the aggregated information initiated from other CHs toward the BS [33] .

Some of the schemes described above have neglected some specifics of WSN structures, including energy-related issues. Most of the previous contributions, which are based on the clustering concept, do not take into account the trade-off between the quality of sensed data, the transmitting power, and the power stored in candidate nodes to select the best routes between the slave sensors and the CH, and they have simplified or ignored the routing issue in the context of Bayesian tracking.

The incorporation of communication costs in the sensor selection approaches leads to the following: (i) a more complex simultaneous optimal sensor and communication path selection, as the communication costs depend on which path the cluster selects, and (ii) creation of a strong interplay between the communication link and the associated estimation at each node. To our knowledge, this problem has not been considered yet in the literature.

Our contribution lies in the following aspects: (1) we improve the use of VF algorithm, which perfectly fits the highly nonlinear conditions and eliminates the transmission error; (2) we investigate the impact of the best candidate sensor selection on the QVF algorithm performances and propose an adaptive quantization scheme; and (3) we adaptively select the optimal communication path to minimize the transmission energy consumption in WSNs.

3. MODELING AND PROBLEM STATEMENT

3.1. Quantized proximity observation model

Consider a wireless sensor network, in which the sensor locations $\boldsymbol{S}^i = (s_1^i, s_2^i)$, $i = 1, 2, \ldots, N_s$ are assumed known, where N_s is the total number of sensors. We are interested in tracking a target position $\boldsymbol{x}_t = (x_{1,t}\ ,\ x_{2,t})^{\mathrm{T}}$ at each instant t ($t = 1, \ldots, N$, where N denotes the number of observations). Around a given position of the target, the CH activates a cell of sensors that transmit only when detecting the presence of the target in their sensing field. Depending on a predictive position of the target, the CH activates the appropriate cell of slave sensors or moves the control to another CH. Consider the activated sensor i (the process of activation is explained in Section 4); its observation γ_t^i is modeled by

$$\gamma_t^i = C\,\|\boldsymbol{x}_t - \boldsymbol{S}^i\,\|^{\eta} + \epsilon_t \tag{1}$$

where ϵ_t is a Gaussian noise with zero mean and known variance σ_ϵ^2. The constants η and C are also assumed to be known. The sensor transmits its observation to the CH only if the target is detected, which is equivalent to the condition that $R_{\min} \leq \|\boldsymbol{x}_t - \boldsymbol{S}^i\,\| \leq R_{\max}$ where $R_{\max}$ ($R_{\min}$) denotes the maximum (minimum) distance at which the sensor can detect the target.

Before being transmitted, the observation is quantized by partitioning the observation space into N_t^i intervals $\mathcal{R}_j = [\tau_j(t), \tau_{j+1}(t)]$, where $j \in \{1, \ldots, N_t^i\}$. N_t^i presents the quantization level ($N_t^i = 2^{L_t^i}$ where L_t^i denotes the number of quantization bits per observation). The quantizer, assumed uniform, is specified through the following: (i) the thresholds $\{\tau_j(t)\}_{j=1}^{j=N_t^i+1}$, where (if $\eta \geq 0$): $\tau_1(t) = KR_{\min}^{\eta}$, $\tau_j(t) \leq \tau_{j+1}(t)$ and $\tau_{N_t^i+1}(t) = KR_{\max}^{\eta}$; and (ii) the quantization rule

$$y_t^i = d_j \text{ if } \gamma_t^i \in [\tau_j(t), \tau_{j+1}(t)] \tag{2}$$

the normalized d_j is given by $d_j = (\tau_j(t) + \Delta/2)/(\tau_{N_{t+1}^i}(t) - \tau_1(t))$ and $\Delta = \tau_{N_t^i+1}(t) - \tau_1(t)/N_t^i$. Then, the signal received by the CH from the sensor i at the sampling instant t is written as

$$z_t^i = \beta_i\ y_t^i + n_t \tag{3}$$

where $\beta_i = r_i^{\psi}$ is the ith sensor channel attenuation coefficient, r_i is the transmission distance between the ith sensor and the CH, ψ is the path-loss exponent, and n_t is a random Gaussian noise sensor with a zero mean and a variance σ_n^2.

3.2. General state evolution model

In this paper, we use a general state evolution model described in [4,34,35]. The augmented state $\boldsymbol{\alpha}_t = (\boldsymbol{x}_t, \boldsymbol{\mu}_t, \boldsymbol{\lambda}_t)$ has a hierarchical model as follows:

$$\left\{ \begin{array}{lcl} \boldsymbol{\mu}_t & \sim & \mathcal{N}(\boldsymbol{\mu}_t|\boldsymbol{\mu}_{t-1}, \bar{\boldsymbol{\lambda}}) \\ \boldsymbol{\lambda}_t & \sim & \mathcal{W}_{\bar{n}}(\boldsymbol{\lambda}_t|\bar{S}) \\ \boldsymbol{x}_t & \sim & \mathcal{N}(\boldsymbol{\mu}_t, \boldsymbol{\lambda}_t) \end{array} \right. \tag{4}$$

where $\boldsymbol{x}_t$ and $\boldsymbol{\mu}_t$ are the target position and its expectation, which are supposed to be Gaussian, and $\boldsymbol{\lambda}_t$ is the precision matrix, which is assumed to have a Wishart distribution. These schemes allow the computation of the posterior distribution $p(\boldsymbol{\alpha}_t|z_{1:t})$, where $z_{1:t} = \{z_1, z_2, \ldots, z_t\}$ denotes observations gathered until t. The next subsection describes the Bayesian estimation approach via a QVF algorithm.

3.3. Overview of the variational filtering algorithm

In this section, we assume that the quantization level is already optimized (Section 4). Hence, the observation model is completely defined. The aim of this section is to describe the target position estimation procedure.

According to model 4, the augmented hidden state is now $\boldsymbol{\alpha}_t = (\boldsymbol{x}_t, \boldsymbol{\mu}_t, \boldsymbol{\lambda}_t)$. We consider the posterior distribution $p(\boldsymbol{\alpha}_t|z_{1:t})$, where $z_{1:t} = \{z_1, z_2, \ldots, z_t\}$ denotes the collection of observations gathered until time t. The variational approach consists in approximating $p(\boldsymbol{\alpha}_t|z_{1:t})$ by a separable distribution $q(\boldsymbol{\alpha}_t) = \Pi_i q(\boldsymbol{\alpha}_t^i)$ that minimizes the Kullback–Leibler (KL) divergence between the true filtering distribution and the approximate distribution,

$$D_{\mathrm{KL}}(q||p) = \int q(\boldsymbol{\alpha}_t) \log \frac{q(\boldsymbol{\alpha}_t)}{p(\boldsymbol{\alpha}_t|z_{1:t})} \mathrm{d}\boldsymbol{\alpha}_t \tag{5}$$

To minimize the KL divergence subject to constraint $\int q(\boldsymbol{\alpha}_t)\mathrm{d}\boldsymbol{\alpha}_t = \Pi_i \int q(\boldsymbol{\alpha}_t^i)\mathrm{d}\boldsymbol{\alpha}_t^i = 1$, the Lagrange multiplier method is used, yielding the following approximate distribution [4,34]:

$$q(\boldsymbol{\alpha}_t^i) \propto \exp \langle \log p(z_t, \boldsymbol{\alpha}_t) \rangle_{\Pi_{j\neq i} q(\boldsymbol{\alpha}_t^j)} \tag{6}$$

where $\langle . \rangle_{q(\boldsymbol{\alpha}_t^j)}$ denotes the expectation operator relative to the distribution $q(\boldsymbol{\alpha}_t^j)$.

With the separable approximate distribution $q(\boldsymbol{\alpha}_{t-1})$ at time $t-1$ taken into account, the filtering distribution $p(\boldsymbol{\alpha}_t|z_{1:t})$ is sequentially approximated according to the following scheme:

$$\begin{aligned} \hat{p}(\boldsymbol{\alpha}_t|z_{1:t}) &= \frac{p(z_t|\boldsymbol{\alpha}_t) \int p(\boldsymbol{\alpha}_t|\boldsymbol{\alpha}_{t-1}) q(\boldsymbol{\alpha}_{t-1}) \mathrm{d}\boldsymbol{\alpha}_{t-1}}{p(z_t|z_{1:t-1})} \\ &\propto p(z_t|\boldsymbol{x}_t) p(\boldsymbol{x}_t|\boldsymbol{\mu}_t, \boldsymbol{\lambda}_t) p(\boldsymbol{\lambda}_t) q_p(\boldsymbol{\mu}_t) \\ \text{with} \quad q_p(\boldsymbol{\mu}_t) &= \int p(\boldsymbol{\mu}_t|\boldsymbol{\mu}_{t-1}) q(\boldsymbol{\mu}_{t-1}) \mathrm{d}\boldsymbol{\mu}_{t-1} \end{aligned} \tag{7}$$

Therefore, through a simple integral with respect to μ_{t-1}, the filtering distribution $p(\boldsymbol{\alpha}_t|z_{1:t})$ can be sequentially updated. Considering the general state evolution model proposed above, the evolution of $q(\mu_{t-1})$ is Gaussian, namely $p(\mu_t|\mu_{t-1}) \sim \mathcal{N}(\boldsymbol{\mu}_{t-1}, \bar{\boldsymbol{\lambda}})$. With the definition of $q(\mu_{t-1}) \sim \mathcal{N}(\boldsymbol{\mu}_{t-1}^*, \boldsymbol{\lambda}_{t-1}^*)$, $q_p(\mu_t)$ is also Gaussian, with the following parameters,

$$\begin{aligned} & q_p(\boldsymbol{\mu}_t) \sim \mathcal{N}(\boldsymbol{\mu}_t^p, \boldsymbol{\lambda}_t^p) \\ & \text{where } \boldsymbol{\mu}_t^p = \boldsymbol{\mu}_{t-1}^* \text{ and } \boldsymbol{\lambda}_t^p = ({\boldsymbol{\lambda}_{t-1}^*}^{-1} + \bar{\boldsymbol{\lambda}}^{-1})^{-1} \end{aligned} \tag{8}$$

The temporal dependence is hence reduced to the incorporation of only one Gaussian component approximation $q_p(\boldsymbol{\mu}_{t-1})$. The update and the approximation of the filtering distribution $p(\boldsymbol{\alpha}_t|z_{1:t})$ are jointly performed, yielding a natural and adaptive compression [34,36]. According to Equation (6), variational calculus leads to the following iterative solution:

$$\begin{array}{lcl} q(\boldsymbol{x}_t) & \propto & p(z_t|\boldsymbol{x}_t)\mathcal{N}(\boldsymbol{x}_t|\langle\boldsymbol{\mu}_t\rangle, \langle\boldsymbol{\lambda}_t\rangle) \\ q(\boldsymbol{\mu}_t) & \propto & \mathcal{N}(\boldsymbol{\mu}_t|\boldsymbol{\mu}_t^*, \boldsymbol{\lambda}_t^*) \\ q(\boldsymbol{\lambda}_t) & \propto & \mathcal{W}_{n^*}(\boldsymbol{\lambda}_t|S_t^*) \\ q(\boldsymbol{\mu}_t|\boldsymbol{\mu}_{t-1}) & \propto & \mathcal{N}(\boldsymbol{\mu}_t^p, \boldsymbol{\lambda}_t^p) \end{array} \tag{9}$$

where the parameters are iteratively updated according to the following scheme:

$$\begin{aligned} \boldsymbol{\mu}_t^* &= \boldsymbol{\lambda}_t^{*-1} \left(\langle\boldsymbol{\lambda}_t\rangle \langle\boldsymbol{x}_t\rangle + \boldsymbol{\lambda}_t^p \boldsymbol{\mu}_t^p \right) \\ \boldsymbol{\lambda}_t^* &= \langle\boldsymbol{\lambda}_t\rangle + \boldsymbol{\lambda}_t^p \\ n^* &= \bar{n} + 1 \\ S_t^* &= \left(\langle \boldsymbol{x}_t \boldsymbol{x}_t^{\mathrm{T}} \rangle - \langle \boldsymbol{x}_t \rangle \langle \boldsymbol{\mu}_t \rangle^{\mathrm{T}} - \langle \boldsymbol{\mu}_t \rangle \langle \boldsymbol{x}_t \rangle^{\mathrm{T}} + \langle \boldsymbol{\mu}_t \boldsymbol{\mu}_t^{\mathrm{T}} \rangle + \bar{S}^{-1} \right)^{-1} \\ \boldsymbol{\mu}_t^p &= \boldsymbol{\mu}_{t-1}^* \\ \boldsymbol{\lambda}_t^p &= \left(\boldsymbol{\lambda}_{t-1}^{*-1} + \bar{\boldsymbol{\lambda}}^{-1} \right)^{-1} \end{aligned} \tag{10}$$

3.4. Predictive distribution calculation

In the Bayesian inference framework, besides updating the filtering distribution $p(\boldsymbol{x}_t|z_{1:t})$, the activated CH also needs to calculate the predictive distribution $p(\boldsymbol{x}_t|z_{1:t-1})$. In fact, the prediction calculation is of great importance for cluster management. The predictive distribution $p(\boldsymbol{x}_t|z_{1:t-1})$ can be efficiently updated by variational inference. Taking into account the separable approximate distribution $q(\boldsymbol{\alpha}_{t-1}) \propto p(\boldsymbol{\alpha}_{t-1}|z_{1:t-1})$, we write the predictive distribution as

$$\begin{aligned} p(\boldsymbol{\alpha}_t|z_{1:t-1}) &\propto \int p(\boldsymbol{\alpha}_t|\boldsymbol{\alpha}_{t-1}) q(\boldsymbol{\alpha}_{t-1}) \mathrm{d}\boldsymbol{\alpha}_{t-1} \\ &\propto p(\boldsymbol{x}_t, \boldsymbol{\lambda}_t|\boldsymbol{\mu}_t) q_p(\boldsymbol{\mu}_t) \end{aligned} \tag{11}$$

The exponential form solution, which minimizes the KL divergence between the predictive distribution $p(\boldsymbol{\alpha}_t|z_{1:t-1})$ and the separable approximate distribution $q_{t|t-1}(\boldsymbol{\alpha}_t)$,

yields Gaussian distributions for the target state and its mean and a Wishart distribution for the precision matrix:

$$\begin{aligned} q_{t|t-1}(\boldsymbol{x}_t) &\propto \mathcal{N}(\langle\boldsymbol{\mu}_t\rangle_{q_{t|t-1}}, \langle\boldsymbol{\lambda}_t\rangle_{q_{t|t-1}}) \\ q_{t|t-1}(\boldsymbol{\mu}_t) &\propto \mathcal{N}(\boldsymbol{\mu}^*_{t|t-1}, \boldsymbol{\lambda}^*_{t|t-1}) \\ q_{t|t-1}(\boldsymbol{\lambda}_t) &\propto \mathcal{W}_{n_x}(\boldsymbol{V}^*_{t|t-1}, n^*_{t|t-1}) \end{aligned} \tag{12}$$

where the hyper-parameters are updated according to the following iterative scheme:

$$\boldsymbol{\mu}^p_t = \boldsymbol{\mu}^*_{t-1} \tag{13}$$

$$\begin{aligned} \boldsymbol{\lambda}^p_t &= ({\boldsymbol{\lambda}^*_{t-1}}^{-1} + \bar{\boldsymbol{\lambda}}^{-1})^{-1} \\ \boldsymbol{\mu}^*_{t|t-1} &= {\boldsymbol{\lambda}^*_{t|t-1}}^{-1}(\langle\boldsymbol{\lambda}_t\rangle_{q_{t|t-1}}\langle\boldsymbol{x}_t\rangle_{q_{t|t-1}} + \boldsymbol{\lambda}^p_t\boldsymbol{\mu}^p_t) \\ \boldsymbol{\lambda}^*_{t|t-1} &= \langle\boldsymbol{\lambda}_t\rangle_{q_{t|t-1}} + \boldsymbol{\lambda}^p_t \\ n^*_{t|t-1} &= \bar{n} + 1 \\ \boldsymbol{V}^*_{t|t-1} &= (\langle\boldsymbol{x}_t\boldsymbol{x}_t^{\mathrm{T}}\rangle_{q_{t|t-1}} - \langle\boldsymbol{x}_t\rangle_{q_{t|t-1}}\langle\boldsymbol{\mu}_t\rangle^{\mathrm{T}}_{q_{t|t-1}} \\ &\quad - \langle\boldsymbol{\mu}_t\rangle_{q_{t|t-1}}\langle\boldsymbol{x}_t\rangle^{\mathrm{T}}_{q_{t|t-1}} + \langle\boldsymbol{\mu}_t\boldsymbol{\mu}_t^{\mathrm{T}}\rangle_{q_{t|t-1}} + \bar{\boldsymbol{V}}^{-1})^{-1} \end{aligned} \tag{14}$$

and the predictive expectations of the target state are now evaluated by the following expressions:

$$\begin{aligned} \langle\boldsymbol{x}_t\rangle_{q_{t|t-1}} &= \langle\boldsymbol{\mu}_t\rangle_{q_{t|t-1}} \\ \langle\boldsymbol{x}_t\boldsymbol{x}_t^{\mathrm{T}}\rangle_{q_{t|t-1}} &= \langle\boldsymbol{\lambda}_t\rangle^{-1}_{q_{t|t-1}} + \langle\boldsymbol{\mu}_t\rangle_{q_{t|t-1}}\langle\boldsymbol{\mu}_t\rangle^{\mathrm{T}}_{q_{t|t-1}} \end{aligned} \tag{15}$$

Compared with the PF method, the variational approximation dramatically reduces the computational cost and the memory requirements in the prediction phase. In fact, the expectations involved in the computation of the predictive distribution have closed forms, avoiding the use of Monte Carlo integration.

3.5. Cluster head determination

The QVF provides, at the sampling instant t, the predicted target position $\boldsymbol{x}_{t/t-1} = \langle\boldsymbol{x}_t\rangle_{q_{t|t-1}}$. As shown in Figure 1, on the basis of this predicted information, the CH CH_{t-1} at sampling instant $t-1$ selects the next CH CH_t. If the predicted target position $\langle\boldsymbol{x}_t\rangle_{q_{t|t-1}}$ remains in the vicinity of CH_{t-1}, which means that at least four of its slave sensors can detect the target, then $CH_t = CH_{t-1}$. Otherwise, if $\langle\boldsymbol{x}_t\rangle_{q_{t|t-1}}$ is going beyond the sensing range of the current cluster, then a new CH_t is activated, on the basis of the target position prediction $\langle\boldsymbol{x}_t\rangle_{q_{t|t-1}}$ and its future tendency.

$$CH_t = \arg\max_{k=1,\ldots,K}\{\frac{\cos\theta^k_t}{d^k_t}\} \tag{16}$$

$$\text{where } d^k_t = \|\langle\boldsymbol{x}_t\rangle_{q_{t|t-1}} - L_{CH^k_t}\|$$

$$\text{and } \theta^k_t = angle(\overrightarrow{\langle\boldsymbol{x}_{t-1}\rangle\langle\boldsymbol{x}_t\rangle_{q_{t|t-1}}}, \overrightarrow{\langle\boldsymbol{x}_{t-1}\rangle L_{CH^k_t}})$$

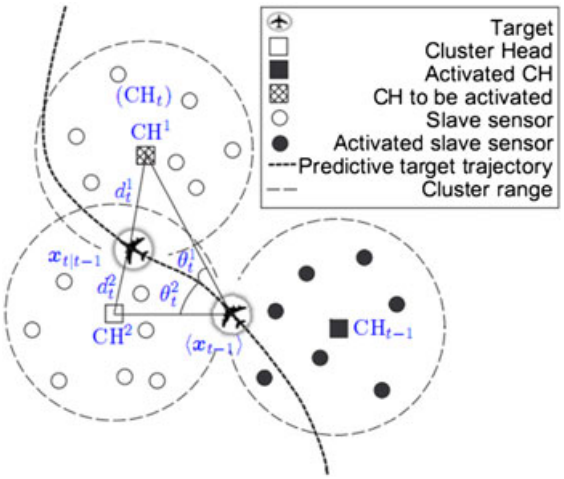

Figure 1. Prediction-based CH_t activation.

where K is the number of CHs in the neighborhood of CH_{t-1} and $L_{CH^k_t}$ is the location of the kth neighboring CH_t.

As illustrated in Figure 1, the traditional cluster activation rule [37] activates CH^2 to update the filtering distribution at time t because it is the closest CH to the target prediction $\boldsymbol{x}_{t|t-1}$. But according to the tendency, the target is very likely to go out of its vicinity in a short time, causing unnecessary hand-off operations. From the decision rule described by Equation (16), it is CH^1 that is activated, as the target is most likely detected by it and would stay in its vicinity for a longer period. With the future tendency of the target taken into consideration, the non-myopic cluster activation rule avoids unnecessary hand-off operations compared with the traditional one. Therefore, the target tracking accuracy is ensured, and the energy consumption is minimized as well. Thanks to the variational calculus, communication between CH_{t-1} and CH_t is limited to simply sending the mean and the precision of $q(\boldsymbol{\mu}_{t-1})$. Therefore, the cluster-based VF algorithm outperforms the classical distributed PF algorithm in resource (energy, bandwidth, and memory) savings, as a large number of particles and corresponding weights are maintained and propagated in the latter case. With respect to the tracking accuracy, the VF and PF algorithms approximate the true state distribution in different ways. When calculating the integral involved in the Bayesian filtering, the PF uses a large amount of particles whereas the VF introduces hidden variables to bypass the difficulty. These random variables introduced by the VF act as links that connect the observations to the unknown parameters via Bayes law. The error propagation problem is dramatically reduced as approximation of the filtering distribution is performed during observation incorporation.

To sum up, this CH determination method yields several advantages. Firstly, the cost of hardware configuration

drops sharply owing to the low cost of slave sensors. Secondly, the required bandwidth and the consumed energy in communication are dramatically reduced. Because the signal processing task is assigned to only one activated CH, only the slave sensors belonging to the active CH are required to transmit their observations over short distances. In addition, avoiding CH competition puts an end to unnecessary resource consumption. Only when the hand-off operation occurs does the active CH need to communicate the temporal dependence information to the subsequent CH. However, the occurrence of hand-off operations is reduced by the nonmyopic selective CH activation rule. Furthermore, the temporal dependence information is reduced by the VF algorithm to only the parameters of a Gaussian distribution. The limitation of this strategy lies in its vulnerability to external attack. In fact, the activated CH is the only sensor performing tracking algorithm, and none of its slave sensors would be able to take over this task.

The next section is devoted to the proposed method for selecting the candidate sensors that participate in target tracking.

4. MAXIMUM MUTUAL INFORMATION UNDER ENERGY CONSTRAINTS-BASED SENSOR SELECTION APPROACH

Because the predicted target position $\boldsymbol{x}_p(t) = \langle \boldsymbol{x}_t \rangle_{q_{t+1|t}}$ at time t is available, it could be used to select the optimal communication route. The sensors inside the disk centered at $\boldsymbol{x}_p(t)$ with radius $R_{\max}$ are selected, and CH is elected according to Equation (16). A sensor node communicates with CH through the selected route including direct and indirect links. The selected route will be taken according to the best communication procedure. The best communication path selection scheme allows CH to get the best copy of the source signal transmitted by the source sensor. The CH computes for each communication link "sensor–CH" a multi-criteria function (detailed in Section 4.1) and selects the optimal communication route, which has the highest MI under energy and node density constraints.

In the next subsection, we detail this criterion and the parameters taken into consideration in order to select the best communication route between the candidate sensor nodes and the CH.

4.1. Maximum mutual information under energy constraints criterion

The main idea of this criterion for sensor selection is to define the main parameters that may influence the relevance of the sensors cooperation, which are the following: (1) information that can be transferred from candidate sensor i, $\boldsymbol{MI}(\boldsymbol{x}_t, z_t^i)$ (detailed in Section 4.2); (2) its energy ($\boldsymbol{E}$(i)) (detailed in Section 4.3); (3) the transmitting energy between one sensor and the CH $\boldsymbol{P}(i)$ (detailed in Section 4.4); and (4) its density ($\boldsymbol{D}$(i)) (detailed in Section 4.5). The problem is how to formulate this criterion for the CH to select the best sensor that provides satisfied data of the target and balances the energy level among all sensors and minimum node density in a local cluster. The criterion function for node i is given by

$$\begin{aligned} \arg \max_{i=1,\ldots,C} \ & \boldsymbol{MI}(\boldsymbol{x}_t, z_t^i) \\ & \text{s.t}\, \boldsymbol{P}(i) < P_0 \\ & \text{s.t}\, \boldsymbol{E}(i) > E_0 \\ & \text{s.t}\, \boldsymbol{D}(i) < D_0 \end{aligned} \tag{17}$$

where P_0, E_0, and D_0 (predefined thresholds) are the maximum power, the minimum energy, and the maximum density of node constraints, respectively. C represents the set of all pre-selected sensors.

4.2. Computation of the mutual information function

The MI function is often used to measure the efficiency of a given information. The MI function is a quantity measuring the amount of information that the observable variable z_t carries about the unknown parameter $\boldsymbol{x}_t$. The MI between the observation z_t^i and the source $\boldsymbol{x}_t$ is proportional to

$$MI(\boldsymbol{x}_t, z_t^i) \ \propto \ p(z_t^i|\boldsymbol{x}_t) \log(p(z_t^i|\boldsymbol{x}_t)) \tag{18}$$

The likelihood function (L) is expressed as

$$\begin{aligned} L(\boldsymbol{s}^i) &= p(z_t^i|\boldsymbol{x}_t) \\ &= \sum_{j=0}^{N_t^i-1} p\left(\tau_j(t) < \gamma_t^i < \tau_{j+1}(t)\right) \mathcal{N}\left(h_t^i d_j, \sigma_\epsilon^2\right) \end{aligned} \tag{19}$$

where

$$p\left(\tau_j(t) < \gamma_t^i < \tau_{j+1}(t)\right) = \int_{\tau_j(t)}^{\tau_{j+1}(t)} \mathcal{N}\left(\rho_{\gamma_t^i}(\boldsymbol{s}^i), \sigma_n^2\right) \mathrm{d}\gamma_t \tag{20}$$

is computed according to the quantization rule defined in Equation (2), in which

$$\rho_{\gamma_t^i}(\boldsymbol{s}^i) = K \|\boldsymbol{x}_t - \boldsymbol{s}^i\|^\eta \tag{21}$$

It is worth noting that the expression of the MI given in Equation (18) depends on the target position $\boldsymbol{x}_t$ at the sampling instant t and on the activated sensor i. However, as the target position is unknown, the MI is replaced by its expectation according to the predictive distribution $p(\boldsymbol{x}_t|z_{1:t-1}^i)$ of the target position:

$$< MI(\boldsymbol{s}^i) > = \ E_{p(\boldsymbol{x}_t|z_{1:t-1}^i)}\left[MI(\boldsymbol{s}^i)\right] \tag{22}$$

Computing the above expectation is analytically untractable. However, as the VF algorithm yields a Gaussian predictive distribution $\mathcal{N}(\boldsymbol{x}_t; \boldsymbol{x}_{t/t-1}, \lambda_{t/t-1})$, expectation (22) can be efficiency approximated by a Monte Carlo scheme:

$$< MI(\boldsymbol{s}^i) > \simeq \frac{1}{J} \sum_{j=1}^{J} MI(\tilde{\boldsymbol{x}}_t^j, \boldsymbol{s}^i),$$
$$\tilde{\boldsymbol{x}}_t^j \sim \mathcal{N}(\boldsymbol{x}_p(t); \boldsymbol{x}_{t/t-1}, \boldsymbol{\lambda}_{t/t-1})$$

where $\tilde{\boldsymbol{x}}_t^j$ is the jth drawn sample at instant t and J is the total number of drawn vectors $\tilde{\boldsymbol{x}}_t$.

4.3. Computation of the lifetime energy

The energy $\boldsymbol{E}$ is an important parameter in a resource-limited network such as the WSN. It is generally seen as the most important parameter. Indeed, the remaining battery level appears to be the most important thing in this parameter, but it is not the only one; it is given by

$$\boldsymbol{E}(i) = \boldsymbol{A}(i) \times \mathbf{APS} \tag{23}$$

where $\boldsymbol{E}(i)$ is the energy parameter of the sensor i, $\boldsymbol{A}$ is the available or remaining power in the battery, and **APS** is the administrator power strategy parameter, which is a percentage defined by the administrator depending on the application. As presented in Equation (23), the energy $\boldsymbol{E}$ could be just the remaining battery level if no administrator power strategy has been defined ($\mathbf{APS} = 1$). In addition, the lower the **APS**, the longer is the lifetime of the WSN.

4.4. Computation of the sensor node transmitting power

The total amount of required transmission power used by the ith sensor within a cluster [38] is proportional to

$$\begin{aligned} P^i(t) &\propto d_i^{\lambda}(N_t^i - 1) \\ &\equiv \| \boldsymbol{s}^i - L_{CH_t} \|^{\lambda} (N_t^i - 1) \end{aligned} \tag{24}$$

where d_i is the transmitting distance (meters) between the CH and the ith sensor, L_{CH_t} is the location of the CH at the sampling instant t, and λ is the path-loss exponent.

4.5. Computation of the density of nodes

The network density varies from one deployment to another and from one node to another within the same deployment depending on the node distribution. Indeed, the more an agent has neighbors the less is the importance of its cooperation. For simplicity's sake, the density $\boldsymbol{D}(i)$ for sensor i is computed by

$$\boldsymbol{D}(i) = \frac{N_{\text{th}}^i}{N_{\text{re}}^i} \tag{25}$$

where N_{th} is the theoretical number of nodes and it is given from the ideal distribution of the nodes or the grid distribution. N_{th} corresponds to the number of nodes within the $R_{\max}$ range. N_{re} is the number of the one-hop neighbors, which means the nodes within the radio range of the node in question.

The next section is devoted to the developed method aimed at adaptively selecting the best communication path between the candidate sensor and the CH.

5. BEST COMMUNICATION PATH SELECTION METHOD

In this section, we assume that sensor selection and CH determination are already optimized (Sections 2 and 3). The aim of this section is to select the best communication path as well as the highest signal-to-noise ratio (SNR) at the CH by considering the two-hop transmission.

5.1. System model

Figure 2 illustrates the idea of the proposed model. The communication is established between a sensor node and the CH through the selected relay including direct and indirect links. The selected relay is achieved according to the optimal communication procedure. The CH can get the best copy of the source signal transmitted by the source sensor S, via the optimal communication path selection scheme. The first one is from the source sensor (direct link), whereas the second one is from the best path as shown in Figure 2. The parameter α_i shown in Figure 2 is the channel coefficient between the source sensor S and the ith sensor. α_i and α_j and β_i and β_j are the flat Rayleigh fading coefficients, which are mutually independent and nonidentical for all i and j.

The signal is simply amplified, at the relay sensor i, using the gain $g = 1/\sqrt{E_s \alpha_i^2 + N_\epsilon}$, where E_s is the transmitted signal energy of the source. It is easy to prove that the source to CH SNR of the indirect path, $S \longmapsto i \longrightarrow$

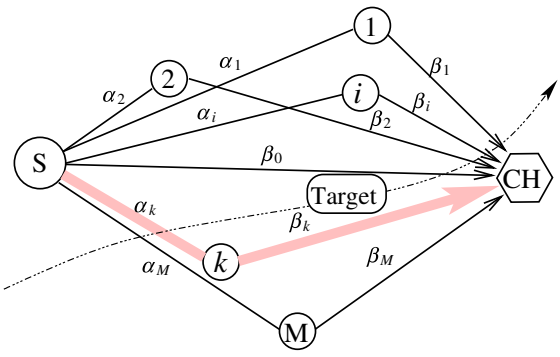

Figure 2. Illustration of the diversity network with the optimal communication path selection scheme.

CH, can be written as

$$\gamma_{S\to i\to CH} = \frac{\gamma_{\alpha_i}\gamma_{\beta_i}}{\gamma_{\alpha_i} + \gamma_{\beta_i} + 1} \tag{26}$$

where $\gamma_{\alpha_i} = \alpha_i^2(E_s/N_\epsilon)$ is the instantaneous SNR of the source signal at the sensor i, $\gamma_{\beta_i} = \beta_i^2(E_i/E_0)$ is the instantaneous SNR of the sensor signal (sensor i) measured at the CH, and E_i is the signal-transmitted energy of the relay i.

The optimal communication path will be selected as the path that achieves the highest source-to-end SNR of indirect and direct paths. The SNR for the best path is given by

$$\gamma_b = \max(\gamma_{\beta_0}, \gamma_{S\to i\to CH})_{i=1\ldots M} \tag{27}$$

where $\gamma_{\beta_0} = \beta_0^2(E_s/N_n)$ is the instantaneous SNR between the source and the CH and M is the total number of links inside the cluster. The upper bound of $\gamma_{S\to i\to CH}$ is given by [39]. Computing the above expression is analytically untractable. However, Equation (27) can be efficiency approximated [40] by

$$\gamma_{S\to i\to CH} \le \gamma_i = \min(\gamma_{\alpha_i}\gamma_{\beta_i}) \tag{28}$$

This approximation simplifies the derivation of the SNR statistics: cumulative distribution function, probability distribution function (PDF), and moment-generating function (MGF).

The next section is devoted to the developed method aimed at adaptively selecting the best communication path between the candidate sensor and the CH.

5.2. Error performance analysis

The error probability p_e of the best path is given as

$$p_e(\gamma_{\beta_0}, \gamma_b) = A erfc\left(\sqrt{B\max(\gamma_{\beta_0}, \gamma_b)}\right) \tag{29}$$

where $erfc(x) = 2/\sqrt{\pi}\int_x^\infty \exp(-t^2)\mathrm{d}t$ and A and B are dependent on the modulation type. Over the random variables representing the SNR values of the optimal communication path, the average error probability is given by

$$P_E = \int_0^\infty p_e(\gamma_b) f_{\gamma_b}\mathrm{d}\gamma_b \tag{30}$$

using the alternative definition of the $erfc(x)$ function as [41]

$$erfc(x) = \frac{2}{\pi}\int_0^{\frac{\pi}{2}} \exp\left(-\frac{x^2}{\sin^2\theta}\right)\mathrm{d}\theta \tag{31}$$

and by substituting Equation (31) into Equation (30), we obtain

$$\begin{aligned} P_E &= \int_0^\infty \frac{2}{\pi}\int_0^{\frac{\pi}{2}} \exp\left(-\frac{B\gamma_b}{\sin^2\theta}\right) f_{\gamma_b}(\gamma_b)\mathrm{d}\gamma_b \\ &= \frac{2}{\pi}\int_0^{\frac{\pi}{2}} M_{\gamma_b}\left(\frac{B}{\sin^2\theta}\right)\mathrm{d}\theta \end{aligned} \tag{32}$$

where $M_{\gamma_b} = \int_0^\infty f_{\gamma_b}(\gamma_b)\exp(-s\gamma_b)\mathrm{d}\gamma_b$ is the MGF of γ_b and f_{γ_b} is the PDF of γ_b.

In order to find the P_E, it is necessary to find the PDF and the MGF of γ_b. We can write the cumulative distribution function of γ_b as follows:

$$\begin{aligned} F_{\gamma_b}(\gamma) &= P(\gamma_b \le \gamma) = P(\gamma_i \le \gamma)P(\gamma_{\beta_0} \le \gamma)_{i=1\ldots M} \\ &= \left[\prod_{i=1}^{M}\left(1 - e^{-\gamma/\gamma_i}\right)\right]\left(1 - e^{-\gamma/\gamma_{\beta_0}}\right) \end{aligned} \tag{33}$$

Assuming that $\gamma_{M+1} = \gamma_{\beta_0}$, the PDF can be computed using the derivative of Equation (33) according to γ, so $f_{\gamma_b}(\gamma)$ can be written as

$$\begin{aligned} f_{\gamma_b}(\gamma) = \sum_{n=1}^{M+1}(-1)^{(n+1)} \sum_{k_1=1}^{M-n+2} \sum_{k_2=k_1+1}^{M-n+3} \cdots \\ \sum_{k_n=k_{n-1}+1}^{M+1} \prod_{j=1}^{n}(e^{-\gamma/\overline{\gamma}_{k_j}}) \sum_{j=1}^{n}\left(\frac{1}{\overline{\gamma}_{k_j}}\right) \end{aligned} \tag{34}$$

By using the PDF in Equation (34), we can write the MGF as

$$\begin{aligned} M_{\gamma_b}(s) = \int_0^\infty e^{-s\gamma} \sum_{n=1}^{M+1}(-1)^{(n+1)} \sum_{k_1=1}^{M-n+2} \sum_{k_2=k_1+1}^{M-n+3} \cdots \\ \sum_{k_n=k_{n-1}+1}^{M+1} \prod_{j=1}^{n}(e^{-\gamma/\overline{\gamma}_{k_j}}) \sum_{j=1}^{n}\left(\frac{1}{\overline{\gamma}_{k_j}}\right)\mathrm{d}\gamma \end{aligned} \tag{35}$$

and the integral can be evaluated in a closed form as

$$\begin{aligned} M_{\gamma_b}(s) = \sum_{n=1}^{M+1}(-1)^{(n+1)} \sum_{k_1=1}^{M-n+2} \sum_{k_2=k_1+1}^{M-n+3} \\ \sum_{k_n=k_{n-1}+1}^{M+1} \frac{\Psi_n}{s+\Psi_n} \end{aligned} \tag{36}$$

where $\Psi_n = \sum_{j=1}^{n}(1/\overline{\gamma}_{k_j})$.

Substituting Equation (36) in Equation (32) and finalizing the integration using [42], we can write P_E in a closed

form as follows:

$$P_{\mathrm{E}} = A \sum_{n=1}^{M+1} (-1)^{(n+1)} \sum_{k_1=1}^{M-n+2} \sum_{k_2=k_1+1}^{M-n+3} \sum_{k_n=k_{n-1}+1}^{M+1} \left(1 - \sqrt{\frac{B/\Psi_n}{1+1/\Psi_n}}\right) \tag{37}$$

Outage analysis quantifies the level of performance that is guaranteed with a certain level of reliability. Probability outage P_{out} is defined as the probability that the channel average MI (I) falls below the required rate R. For the best-path selection diversity networks, P_{out} can be written as

$$P_{\mathrm{out}} = Pr(I \le R) = Pr\left(\frac{1}{2}\log_2(1+\gamma_b) \le R\right)$$
$$= Pr\left(\gamma_b \le 2^{2R} - 1\right) = M_{\gamma_b}\left(2^{2R} - 1\right)$$

The scheme discussed previously will be referred to as adaptive QVF algorithm; its procedure is summarized in Algorithm 1.

Algorithm 1 Pseudo-code of the proposed algorithm

Initialization:

(1) Select the candidate sensors that exist within the $R_{\max}$ range.
(2) Select the best communication path between the candidate sensors and the CH according to Section 5.
(3) Quantize sensors' measurements.
(4) Execute the QVF algorithm.

Iterations:

(1) Select sensors that exist within the $R_{\max}$ range.
(2) Compute the predicted target distribution.
(3) Compute the MI function based on the predicted target position using Equation (18).
(4) Select the optimal candidate sensors according to Section 4.
(5) Select the best communication path between the candidate sensors and the CH according to Section 5.
(6) Quantize sensors' measurements.
(7) Execute the QVF algorithm.

6. SIMULATION RESULTS ANALYSIS

The performance of the proposed algorithms is quantified by four criteria:

(1) The tracking accuracy
(2) The root mean square errors (RMSE) between the estimation and the true trajectory of the mobile target
(3) The execution time
(4) The energy expenditure during the whole tracking process

The system parameters considered in the following simulations are as follows: $\eta = 2$ for free space environment, the

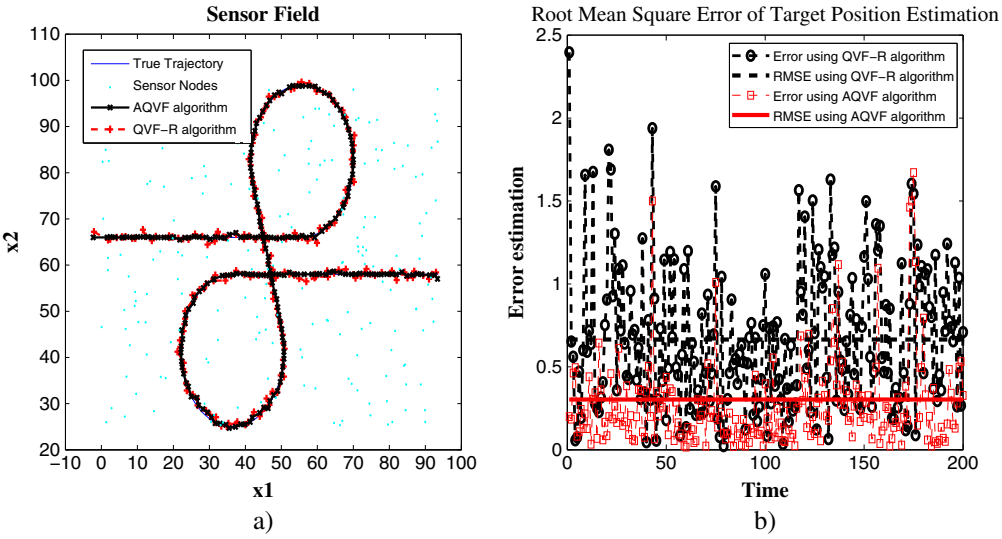

Figure 3. (a) Tracking accuracy between quantized variational filtering (QVF)-R algorithm and the proposed method. (b) Root mean square error (RMSE) comparison between QVF-R algorithm and the proposed method. AQVF, adaptive QVF.

constant characterizing the sensor range is fixed for simplicity to $C = 1$, the CH noise power is $\sigma_n^2 = 10^{-3}$, the total number of sensors is $N_s = 200$, the total sampling instants is $N = 200$, the sensor noise power is $\sigma_\epsilon^2 = 10^{-4}$, the maximum sensing range $R_{\max}$ (the minimum sensing range $R_{\min}$) is fixed to 8.5 m (0 m), and 200 particles were used in QVF, binary VF (BVF), and quantized PF (QPF) algorithms. All sensors have equal initial battery energies of $E_i = 1$ J. All the simulations shown in this paper are implemented with MATLAB version 7.1, using a personal computer with an Intel Pentium 3.4-GHz CPU and 1.0-G RAM.

The approach that uses the QVF algorithm with activating sensors in the circle of radius $R_{\max}$ for target tracking is referred to as QVF-R.

In the following, we compare the tracking accuracy of the proposed algorithm, with those of the QVF-R algorithm, the BVF algorithm [34], and the centralized QPF algorithm [43]. The quantized proximity observation model, formulated in Equation (2), was adopted for the QPF algorithm. One can notice from Figure 3a that, even with abrupt changes in the target trajectory, the desired quality is achieved by the proposed method and outperforms the QVF-R algorithm. Figure 3b compares their

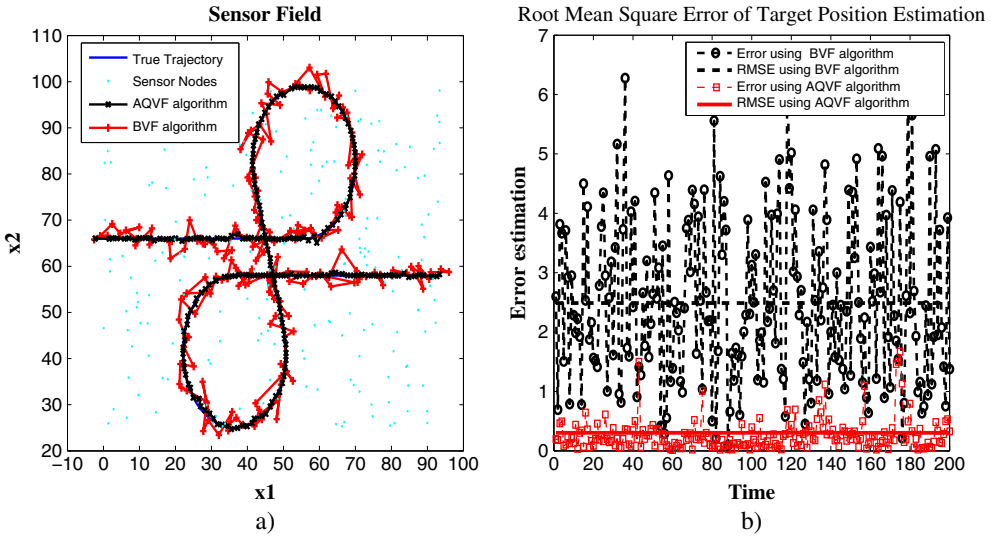

Figure 4. (a) Tracking accuracy between binary variational filtering (BVF) algorithm and the proposed method. (b) Root mean square error (RMSE) comparison between BVF algorithm and the proposed method.

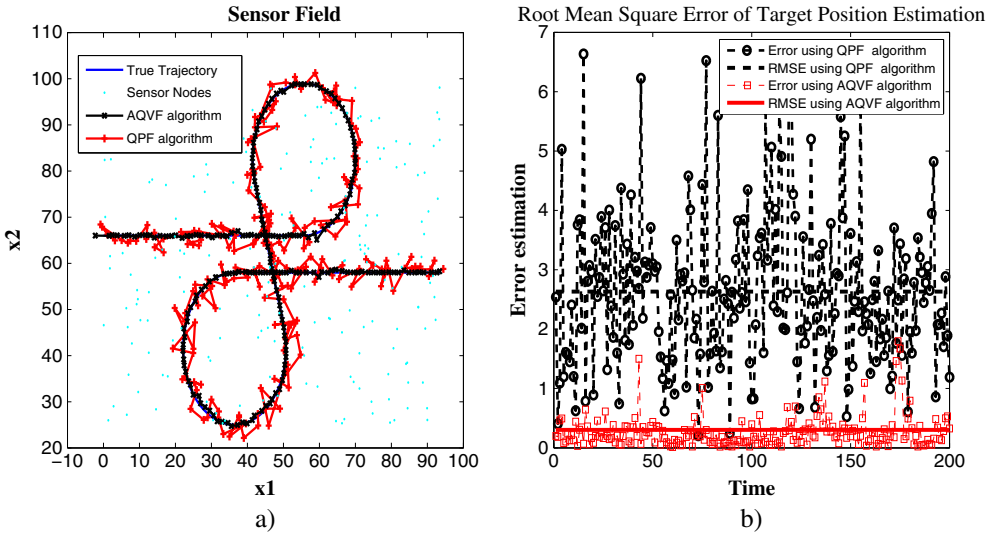

Figure 5. (a) Tracking accuracy between quantized particle filtering (QPF) algorithm and the proposed method. (b) Root mean square error (RMSE) comparison between QPF algorithm and the proposed method. AQVF, adaptive quantized variational filtering.

tracking accuracies in terms of RMSE. The performances of the proposed method demonstrate the effectiveness of the sensor selection approach.

$$RMSE = \sqrt{E\left((x - \widehat{x})^2\right)} \tag{38}$$

where x ($\widehat{x}$) is the true trajectory (the estimated trajectory).

The proposed method and BVF algorithm performances are compared in Figure 4. The results confirm the impact of neglecting the information relevance of sensor measurements, when we used binary proximity sensors. As can be expected, with the amount of particles increasing, the QPF algorithm demonstrates much more accurate tracking at the cost of a higher computation complexity. In particular, the computation time grows proportionally to the increment of the number of particles. The tracking accuracy of QPF algorithm is compared with that of the proposed method in Figure 5. The smaller RMSE of the proposed method in comparison with the QPF method confirms once again the effectiveness of the proposed method in terms of tracking accuracy and the efficiency in non-Gaussian context.

6.1. Root mean square error analysis

The RMSE of the above algorithms may depend on several factors such as the transmitting power between the candidate sensors and the CH, the node density, the sensing range, the path losses, and the sensor noise variances. The purpose of this subsection is to study the impact of these factors when comparing the performance of the above-mentioned tracking algorithms. Figure 6a shows the variation of the RMSE with respect to the node density varying in $\{50, \ldots, 200\}$. As can be expected, the RMSE decreases

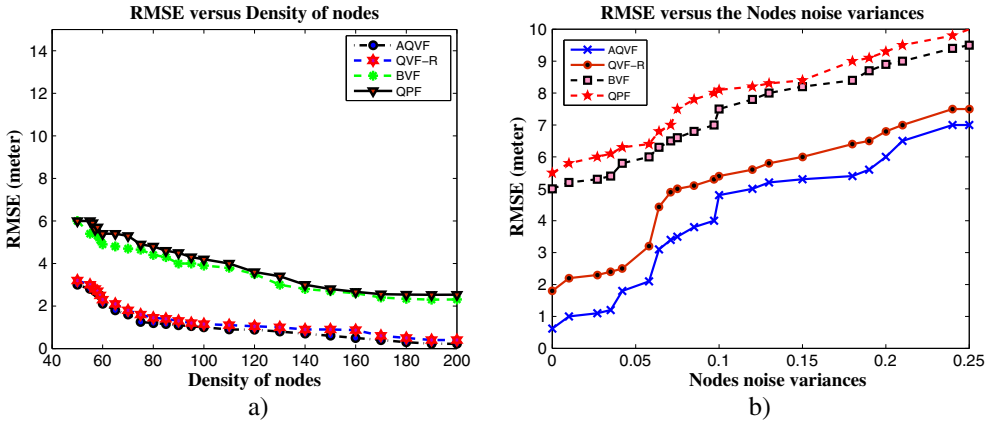

Figure 6. (a) Root mean square error (RMSE) versus node density varying in $\{50, \ldots, 200\}$. (b) RMSE versus node noise variances varying in $\{0, \ldots, 0.25\}$. QVF, quantized variational filtering; BVF, binary variational filtering; QPF, quantized particle filtering.

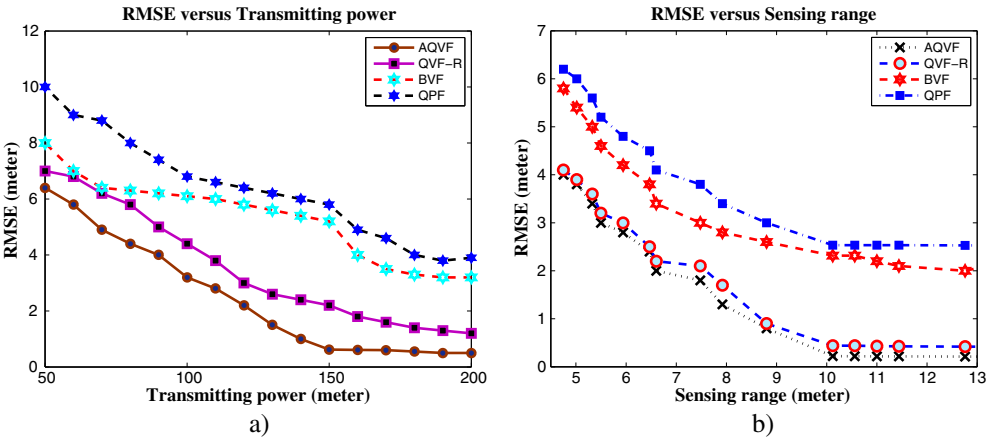

Figure 7. (a) Root mean square error (RMSE) versus transmitting power varying in $\{50, \ldots, 200\}$. (b) RMSE versus sensing range varying in $\{5, \ldots, 13\}$. QVF, quantized variational filtering; BVF, binary variational filtering; QPF, quantized particle filtering.

for all the algorithms when the node density increases. One can also note that the proposed adaptive QVF technique outperforms all the other techniques when varying the node density. It is also worth noting that its RMSE decreases more sharply than those of the other filtering techniques. Figure 6b plots the RMSE versus the node noise variances varying in $\{0, \ldots, 0.25\}$, and Figure 7a plots the RMSE with respect to the nodes transmitting power (varying in $\{50, \ldots, 200\}$). From Figure 7b, we can show that when the sensing range varies in $\{5, \ldots, 13\}$, the error estimation decreases. These results confirm that the proposed method outperforms the classical algorithms when varying the simulation conditions.

Figure 8a shows the bit error rate for binary phase shift keying with different numbers of paths sensors–CH (M). As can clearly be seen in high-SNR regime, the improvement of bit error rate is proportional to the number of sensors–CH links (M). Figure 8b shows the probability outage (P_{out}) performance for $R = 1$ bit/s/Hz.

To evaluate the performances of the proposed method in terms of energy consumption, we have used the model proposed in [44], in which we assume the following: (i) the

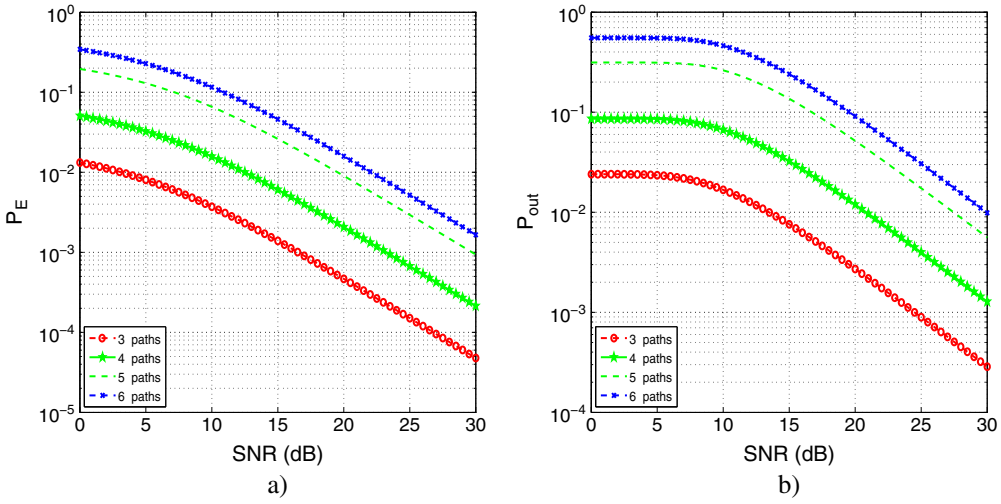

Figure 8. (a) Error performance for the best-path selection scheme over Rayleigh fading channels. (b) Outage performance for the best-path selection scheme over Rayleigh fading channels. SNR, signal-to-noise ratio.

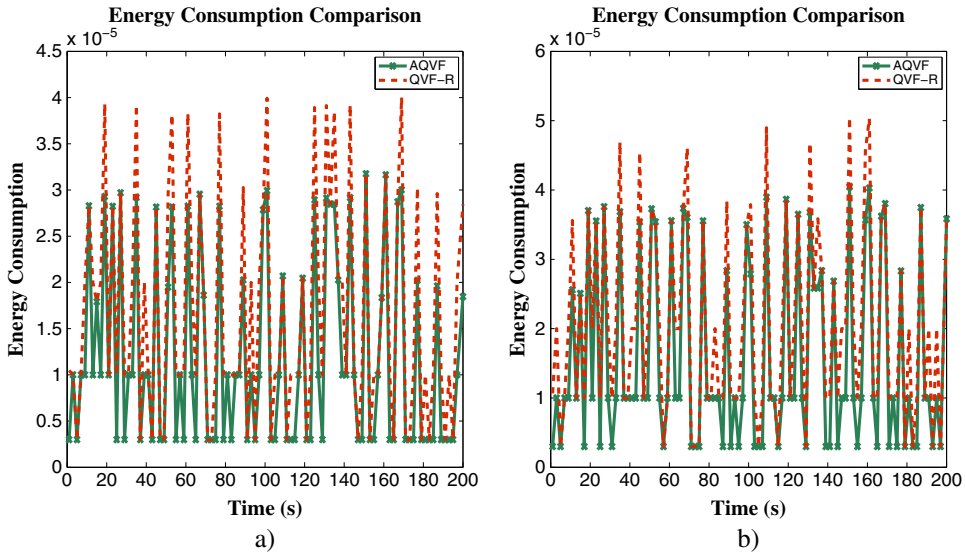

Figure 9. Energy consumption comparison between adaptive quantized variational filtering (AQVF) and quantized variational filtering (QVF)-U algorithms for (a) $L = 3$ and (b) $L = 4$.

Table I. Comparison of target tracking algorithms

Comparison	RMSE (m)	Execution time (s)
AQVF algorithm	0.3011	1.5938
QVF-R algorithm	0.6212	2.3438
BVF algorithm	2.49	2.6563
QPF algorithm	2.632	1.1273

RMSE, root mean square error; AQVF, adaptive quantized variational filtering; QVF, quantized variational filtering; BVF, binary variational filtering; QPF, quantized particle filtering.

communication between the active sensors is via single hop and (ii) the energy consumed in scheduling and computing can be neglected relative to the energy consumed during communications.

The communication energy consists of three components: transmitter electronics energy, radio energy, and receiver electronics energy. The transmit power consumed at sensor (i), while transmitting data to CH, is given by

$$E_T = \epsilon_e + L^i \epsilon_a \beta_i \tag{39}$$

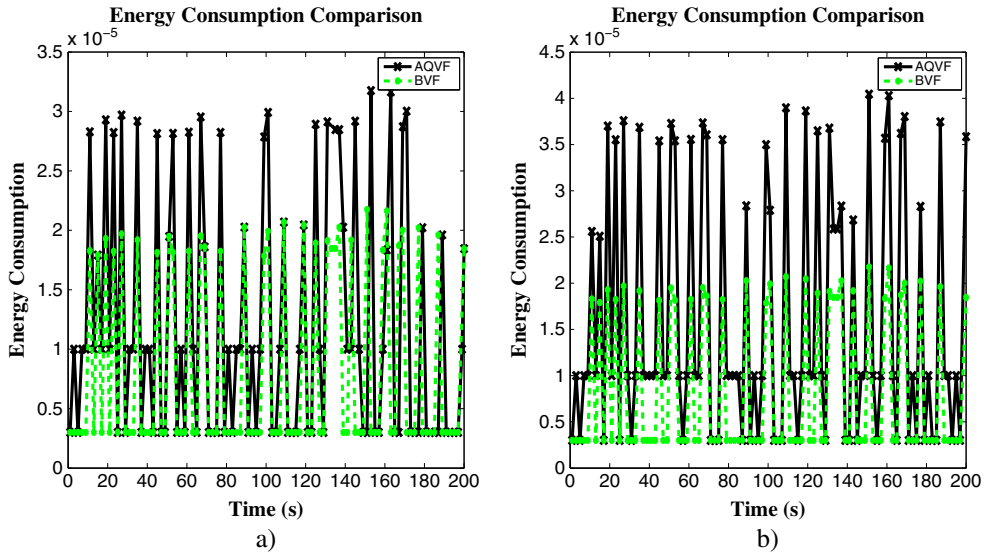

Figure 10. Energy consumption comparison between adaptive quantized variational filtering (AQVF) and binary variational filtering (BVF) algorithms for (a) $L = 3$ and (b) $L = 4$.

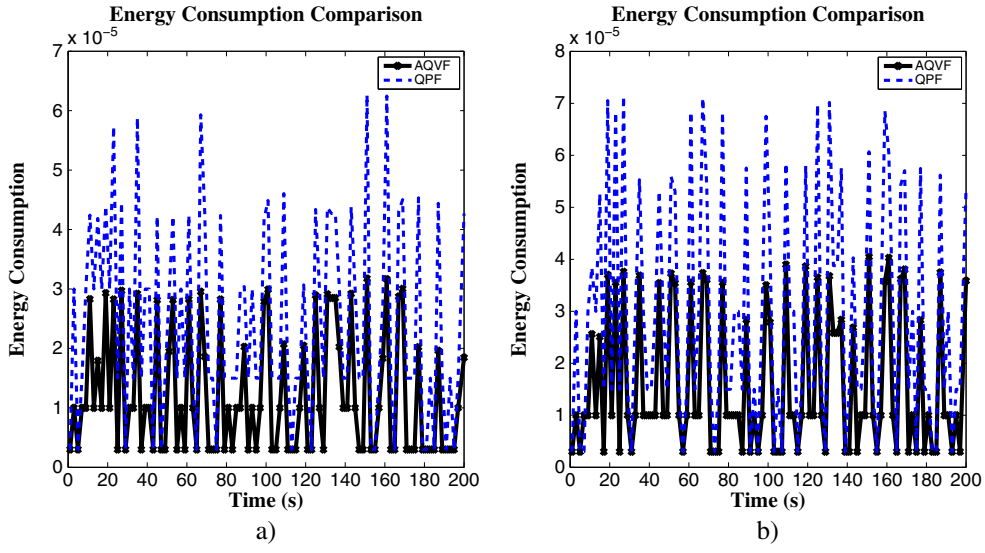

Figure 11. Energy consumption comparison between adaptive quantized variational filtering (AQVF) and quantized particle filtering (QPF) algorithms for (a) $L = 3$ and (b) $L = 4$.

where ϵ_a is the energy dissipated in Joules per bit per square meter and ϵ_e is the energy consumed by the circuit per bit.

The receiving power consumed at ith sensor when receiving data from the CH is given by

$$E_R = L^i \epsilon_r \tag{40}$$

Similarly, the power consumed in sensing is defined by

$$E_S = L^i \epsilon_s \tag{41}$$

where ϵ_s is the energy expending parameter for sensing L^i bits of data. Considering the energy model, we choose $\epsilon_a = 100$ pJ/bit/m^2, $\epsilon_e = 50$ nJ/bit, $\epsilon_r = 135$ nJ/bit, $\epsilon_s = 50$ nJ/bit [34].

From Figures 9–11, we can see that our protocol successfully balances the trade-off between the energy consumption even with several abrupt changes in the trajectory where the bit quantization number is $L = 3$ and $L = 4$. These results confirm that the proposed method outperforms the classical algorithms in terms of energy expenditure during the whole tracking process.

Table I shows the computation complexity, evaluated by the execution time of the algorithm.

7. CONCLUSIONS

In this paper, we considered an optimal sensor and best communication path selection approach for target tracking in WSN with quantized measurements. As for economical reasons, in the hardware layer, the deployment of quantized sensors greatly saves energy; in the software layer, the proposed algorithm decreases the information exchanged between sensors. The proposed method provides not only the estimate of the target position using the QVF algorithm but also proposes an efficiency candidate sensor selection method and a best communication path selection scheme. The sensor selection approach is based on MI maximization under energy constraints that define the main parameters that may influence the relevance of the sensor cooperation for target tracking, whereas the best communication path is selected as well as the highest SNR at the CH. The computation of criteria is based on the target position predictive distribution provided by the QVF algorithm.

APPENDIX A: VARIATIONAL CALCULUS

Assuming that the approximate distribution for the mean $\boldsymbol{\mu}_{t-1}$ follows a Gaussian model ($q(\boldsymbol{\mu}_{t-1}) \sim \mathcal{N}(\boldsymbol{\mu}^*_{t-1}, \boldsymbol{\lambda}^*_{t-1})$) and taking into account the Gaussian transition of the mean ($p(\boldsymbol{\mu}_t|\boldsymbol{\mu}_{t-1}) \sim \mathcal{N}(\boldsymbol{\mu}_{t-1}, \bar{\boldsymbol{\lambda}})$), we give the predictive distribution of μ_t by

$$\begin{aligned} q_p(\boldsymbol{\mu}_t) &= \int p(\boldsymbol{\mu}_t|\boldsymbol{\mu}_{t-1}) q(\boldsymbol{\mu}_{t-1}) \mathrm{d}\boldsymbol{\mu}_{t-1} \\ &\sim \mathcal{N}(\boldsymbol{\mu}^*_{t-1}, ({\boldsymbol{\lambda}^*_{t-1}}^{-1} + \bar{\boldsymbol{\lambda}}^{-1})^{-1}) \end{aligned} \tag{A.1}$$

Let $\boldsymbol{\mu}_t^p$ and $\boldsymbol{\lambda}_t^p$ respectively denote the mean and the precision of the Gaussian distribution $q_p(\boldsymbol{\mu}_t)$: $q_p(\boldsymbol{\mu}_t) \sim \mathcal{N}(\boldsymbol{\mu}_t^p, \boldsymbol{\lambda}_t^p)$. According to Equation (6), the approximate distribution $q(\boldsymbol{\mu}_t)$ is expressed as

$$\begin{aligned} q(\boldsymbol{\mu}_t) &\propto \exp\langle \log p(z_{1:t}, \boldsymbol{\alpha}_t)\rangle_{q(\boldsymbol{x}_t)q(\boldsymbol{\lambda}_t)} \\ &\propto \exp\langle \log p(\boldsymbol{\alpha}_t|z_t)\rangle_{q(\boldsymbol{x}_t)q(\boldsymbol{\lambda}_t)} \\ &\propto \exp\langle \log p(z_t|\boldsymbol{x}_t) + \log p(\boldsymbol{x}_t|\boldsymbol{\mu}_t, \boldsymbol{\lambda}_t) \\ &\qquad + \log p(\boldsymbol{\lambda}_t) \\ &\qquad + \log q_p(\boldsymbol{\mu}_t)\rangle_{q(\boldsymbol{x}_t)q(\boldsymbol{\lambda}_t)} \end{aligned} \tag{A.2}$$

Therefore,

$$\begin{aligned} q(\boldsymbol{\mu}_t) &\propto q_p(\boldsymbol{\mu}_t) \exp\langle \log p(\boldsymbol{x}_t|\boldsymbol{\mu}_t, \boldsymbol{\lambda}_t)\rangle_{q(\boldsymbol{x}_t)q(\boldsymbol{\lambda}_t)} \\ &\propto q_p(\boldsymbol{\mu}_t) \exp\langle -\frac{1}{2}(\boldsymbol{x}_t - \boldsymbol{\mu}_t)^{\mathrm{T}} \boldsymbol{\lambda}_t (\boldsymbol{x}_t - \boldsymbol{\mu}_t)\rangle_{q(\boldsymbol{x}_t)q(\boldsymbol{\lambda}_t)} \\ &\propto q_p(\boldsymbol{\mu}_t) \exp -\frac{1}{2}\Big\{ tr\Big[\langle \boldsymbol{\lambda}_t\rangle_{q(\boldsymbol{\lambda}_t)} \langle (\boldsymbol{x}_t - \boldsymbol{\mu}_t)^{\mathrm{T}} \\ &\qquad (\boldsymbol{x}_t - \boldsymbol{\mu}_t)\rangle_{q(\boldsymbol{x}_t)}\Big]\Big\} \\ &\propto \exp -\frac{1}{2}\Big[(\boldsymbol{\mu}_t - \boldsymbol{\mu}_t^p)^{\mathrm{T}} \boldsymbol{\lambda}_t (\boldsymbol{\mu}_t - \boldsymbol{\mu}_t^p) - 2\boldsymbol{\mu}_t^{\mathrm{T}} \langle \boldsymbol{\lambda}_t\rangle \\ &\qquad \times \langle \boldsymbol{x}_t\rangle + {\boldsymbol{\mu}_t}^{\mathrm{T}} \langle \boldsymbol{\lambda}_t\rangle \boldsymbol{\mu}_t\Big] \end{aligned} \tag{A.3}$$

yielding a Gaussian distribution $q(\boldsymbol{\mu}_t) = \mathcal{N}(\boldsymbol{\mu}_t^*, \boldsymbol{\lambda}_t^*)$. The first and second derivatives of the logarithm of $q(\boldsymbol{\mu}_t)$ are expressed as

$$\begin{aligned} \frac{\partial \log(q(\boldsymbol{\mu}_t))}{\partial \boldsymbol{\mu}_t} &= -\frac{1}{2}\left[2\boldsymbol{\lambda}_t^p(\boldsymbol{\mu}_t - \boldsymbol{\mu}_t^p) - 2\langle \boldsymbol{\lambda}_t\rangle \langle \boldsymbol{x}_t\rangle \right. \\ &\qquad \left. + 2\langle \boldsymbol{\lambda}_t\rangle \boldsymbol{\mu}_t\right] \\ \frac{\partial^2 \log(q(\boldsymbol{\mu}_t))}{\partial \boldsymbol{\mu}_t \partial {\boldsymbol{\mu}_t}^{\mathrm{T}}} &= -\boldsymbol{\lambda}_t^p - \langle \boldsymbol{\lambda}_t\rangle \end{aligned}$$

The precision $\boldsymbol{\lambda}_t^*$ and the mean $\boldsymbol{\mu}_t^*$ of $q(\boldsymbol{\mu}_t)$ are obtained as follows:

$$\boldsymbol{\lambda}_t^* = \langle \boldsymbol{\lambda}_t\rangle + \boldsymbol{\lambda}_t^p \quad \text{and} \quad \boldsymbol{\mu}_t^* = \boldsymbol{\lambda}_t^{*-1}(\langle \boldsymbol{\lambda}_t\rangle \langle \boldsymbol{x}_t\rangle + \boldsymbol{\lambda}_t^p \boldsymbol{\mu}_t^p) \tag{A.4}$$

The approximate separable distribution corresponding to $\boldsymbol{\lambda}_t$ can be computed following the same reasoning as

above:

$$
\begin{aligned}
q(\boldsymbol{\lambda}_t) &\propto \exp\langle \log p(\boldsymbol{\alpha}_t|z_t)\rangle_{q(x_t)q(\boldsymbol{\mu}_t)} \\
&\propto \exp\langle \log p(z_t|\boldsymbol{x}_t) + \log p(\boldsymbol{x}_t|\boldsymbol{\mu}_t,\boldsymbol{\lambda}_t) + \log p(\boldsymbol{\lambda}_t) \\
&\qquad + \log q_p(\boldsymbol{\mu}_t)\rangle_{q(x_t)q(\boldsymbol{\mu}_t)} \\
&\propto p(\boldsymbol{\lambda}_t)\exp\langle \log p(\boldsymbol{x}_t|\boldsymbol{\mu}_t,\boldsymbol{\lambda}_t)\rangle_{q(x_t)q(\boldsymbol{\mu}_t)} \\
&\propto \mathcal{W}_2(\bar{\boldsymbol{V}},\bar{n})|\boldsymbol{\lambda}_t|^{\frac{1}{2}}\exp -\frac{1}{2}\left\{tr\left[\boldsymbol{\lambda}_t\langle(\boldsymbol{x}_t-\boldsymbol{\mu}_t)^{\mathrm{T}}\right.\right. \\
&\qquad \left.\left.(\boldsymbol{x}_t-\boldsymbol{\mu}_t)\rangle_{q(x_t)q(\boldsymbol{\mu}_t)}\right]\right\} \\
&\propto |\boldsymbol{\lambda}_t|^{\frac{\bar{n}+1-(2+1)}{2}} \\
&\exp -\frac{1}{2}\left\{tr\left[\boldsymbol{\lambda}_t(\langle \boldsymbol{x}_t\boldsymbol{x}_t^{\mathrm{T}}\rangle - \langle \boldsymbol{x}_t\rangle\langle\boldsymbol{\mu}_t\rangle^{\mathrm{T}}\right.\right. \\
&\qquad \left.\left.-\langle\boldsymbol{\mu}_t\rangle\langle\boldsymbol{x}_t\rangle^{\mathrm{T}} + \langle\boldsymbol{\mu}_t\boldsymbol{\mu}_t^{\mathrm{T}}\rangle + \bar{\boldsymbol{V}}^{-1})\right]\right\} \qquad \text{(A.5)}
\end{aligned}
$$

which yields a Wishart distribution $\mathcal{W}_2(\boldsymbol{V}^*, n^*)$ for the precision matrix $\boldsymbol{\lambda}_t$ with the following parameters:

$$
\begin{cases}
n^* = \bar{n} + 1, \\
\boldsymbol{V}^* = (\langle \boldsymbol{x}_t\boldsymbol{x}_t^{\mathrm{T}}\rangle - \langle \boldsymbol{x}_t\rangle\langle\boldsymbol{\mu}_t\rangle^{\mathrm{T}} - \langle\boldsymbol{\mu}_t\rangle\langle\boldsymbol{x}_t\rangle^{\mathrm{T}} \\
\qquad + \langle\boldsymbol{\mu}_t\boldsymbol{\mu}_t^{\mathrm{T}}\rangle + \bar{\boldsymbol{V}}^{-1})^{-1}
\end{cases} \qquad \text{(A.6)}
$$

Finally, the approximate distribution $q(\boldsymbol{x}_t)$ has the following expression:

$$
\begin{aligned}
q(\boldsymbol{x}_t) &\propto \exp\langle \log p(\boldsymbol{\alpha}_t|z_t)\rangle_{q(\boldsymbol{\mu}_t)q(\boldsymbol{\lambda}_t)} \\
&\propto \exp\langle \log p(z_t|\boldsymbol{x}_t) + \log p(\boldsymbol{x}_t|\boldsymbol{\mu}_t,\boldsymbol{\lambda}_t) + \log p(\boldsymbol{\lambda}_t) \\
&\qquad + \log q_p(\boldsymbol{\mu}_t)\rangle_{q(\boldsymbol{\mu}_t)q(\boldsymbol{\lambda}_t)} \\
&\propto p(z_t|\boldsymbol{x}_t)\exp\langle \log p(\boldsymbol{x}_t|\boldsymbol{\mu}_t,\boldsymbol{\lambda}_t)\rangle_{q(\boldsymbol{\mu}_t)q(\boldsymbol{\lambda}_t)} \\
&\propto p(z_t|\boldsymbol{x}_t)\exp -\frac{1}{2}\left\{tr\left[\langle\boldsymbol{\lambda}_t\rangle_{q(\boldsymbol{\lambda}_t)}\langle(\boldsymbol{x}_t-\boldsymbol{\mu}_t)^{\mathrm{T}}\right.\right. \\
&\qquad \left.\left.(\boldsymbol{x}_t-\boldsymbol{\mu}_t)\rangle_{q(\boldsymbol{\mu}_t)}\right]\right\} \\
&\propto p(z_t|\boldsymbol{x}_t)\mathcal{N}(\langle\boldsymbol{\mu}_t\rangle,\langle\boldsymbol{\lambda}_t\rangle) \qquad \text{(A.7)}
\end{aligned}
$$

which does not have a closed form. Therefore, contrary to the cases of the mean $\boldsymbol{\mu}_t$ and the precision $\boldsymbol{\lambda}_t$, in order to compute the expectations relative to the distribution $q(\boldsymbol{x}_t)$, one has to resort to the importance sampling method where samples are generated according to the Gaussian $\mathcal{N}(\langle\boldsymbol{\mu}_t\rangle,\langle\boldsymbol{\lambda}_t\rangle)$ and then weighted according to the likelihood $p(z_t|\boldsymbol{x}_t)$.

REFERENCES

1. Chen Y, Zhao Q. On the lifetime of wireless sensor networks. *IEEE Communications Letters* 2005; **9**(11): 976–978.
2. Julier S, Uhlmann J. Unscented filtering and non-linear estimation. In *Proceedings of the IEEE*, Vol. 92, March 2004; 401–422.
3. Djuric P, Kotecha JZJ, Huang Y, Ghirmai T, Bugallo M, Miguez J. Particle filtering. *IEEE Signal Processing Magazine* September 2003; **20**: 19–38.
4. Snoussi H, Richard C. Ensemble learning online filtering in wireless sensor networks. In *IEEE ICCS International Conference on Communications Systems*, 2006.
5. Teng J, Snoussi H, Richard C. Binary variational filtering for target tracking in wireless sensor networks. In *IEEE/SP 14th Workshop on Statistical Signal Processing 2007 (SSP'07)*, 2007; 685–689.
6. Patwari N, Ash J, Kyperountas S, Hero III A, Moses R, Correal N. Locating the nodes: cooperative localization in wireless sensor networks. *IEEE Signal Processing Magazine* 2005; **22**(4): 54–69.
7. Patwari N, Hero III A, Perkins M, Correal N, O'dea R. Relative location estimation in wireless sensor networks. *IEEE Transactions on Signal Processing* 2003; **51**(8): 2137–2148.
8. Patwari N, Hero A, Costa J. Learning sensor location from signal strength and connectivity. *Secure Localization and Time Synchronization for Wireless Sensor and Ad Hoc Networks* 2007: 57–81.
9. Costa J, Patwari N, Hero III A. Distributed weighted-multidimensional scaling for node localization in sensor networks. *ACM Transactions on Sensor Networks (TOSN)* 2006; **2**(1): 64.
10. Patwari N. Location estimation in sensor networks, *Ph.D. dissertation*, Citeseer, 2005.
11. Zhao F, Shin J, Reich J. Information-driven dynamic sensor collaboration for tracking applications. *IEEE Signal Processing Magazine* 2002; **19**(2): 61–72.
12. Li J, AlRegib G. Rate-constrained distributed estimation in wireless sensor networks. *IEEE Transactions on Signal Processing* 2007; **55**(5 Part 1): 1634–1643.
13. Rubin I, Huang X. Capacity aware optimal activation of sensor nodes under reproduction distortion measures. In *Military Communications Conference 2006 (MILCOM 2006)*, 2006; 1–8.
14. Quan Z, Sayed A. Innovations-based sampling over spatially-correlated sensors. In *IEEE International Conference on Acoustics, Speech and Signal Processing 2007 (ICASSP 2007)*, Vol. 3, 2007.
15. Bian F, Kempe D, Govindan R. Utility-based sensor selection. In *The Fifth International Conference on Information Processing in Sensor Networks 2006 (IPSN 2006)*, 2006; 11–18.
16. Hintz K. A measure of the information gain attributable to cueing. *IEEE Transactions on Systems, Man and Cybernetics* 1991; **21**(2): 434–442.
17. Manyika J, Durrant-Whyte H. *Data Fusion and Sensor Management: A Decentralized Information-Theoretic*

Approach. Prentice Hall PTR: Upper Saddle River, NJ, 1995.

18. Liu J, Reich J, Zhao F. Collaborative in-network processing for target tracking. *EURASIP Journal on Applied Signal Processing* 2003; **2003**: 378–391.
19. Ertin E, Fisher J, Potter L. Maximum mutual information principle for dynamic sensor query problems. In *Information Processing in Sensor Networks*. Springer: Heidelberg, 2003; 558–558.
20. Yao K, Hudson R, Reed C, Chen D, Lorenzelli F. Blind beamforming on a randomly distributed sensor array system. *IEEE Journal on Selected Areas in Communications* 1998; **16**(8): 1555–1567.
21. Chu M, Haussecker H, Zhao F. Scalable information-driven sensor querying and routing for ad hoc heterogeneous sensor networks. *International Journal of High Performance Computing Applications* 2002; **16**(3): 293–313.
22. Wang H, Yao K, Pottie G, Estrin D. Entropy-based sensor selection heuristic for target localization. In *Proceedings of the 3rd International Symposium on Information Processing in Sensor Networks ACM*, 2004; 45.
23. Dong Q. Maximizing system lifetime in wireless sensor networks. In *Fourth International Symposium on Information Processing in Sensor Networks 2005 (IPSN 2005)*, 2005; 13–19.
24. Shah R, Rabaey J. Energy aware routing for low energy ad hoc sensor networks. In *IEEE Wireless Communications and Networking Conference (WCNC)*, Vol. 1. IEEE: Piscataway, NJ, USA, 2002; 350–355.
25. Li Q, Aslam J, Rus D. Online power-aware routing in wireless ad-hoc networks. In *Proceedings of the 7th Annual International Conference on Mobile Computing and Networking, ACM*, 2001; 107.
26. Chang J, Tassiulas L. Maximum lifetime routing in wireless sensor networks. *IEEE/ACM Transactions on Networking (TON)* 2004; **12**(4): 609–619.
27. Liu J, Zhao F, Petrovic D. Information-directed routing in ad hoc sensor networks. In *Proceedings of the 2nd ACM International Conference on Wireless Sensor Networks and Applications, ACM*, 2003; 88–97.
28. Sung Y, Misra S, Tong L, Ephremides A. Cooperative routing for distributed detection in large sensor networks. *IEEE Journal on Selected Areas in Communications* 2007; **25**(2): 471–483.
29. Intanagonwiwat C, Govindan R, Estrin D. Directed diffusion: a scalable and robust communication paradigm for sensor networks. In *Proceedings of the 6th Annual International Conference on Mobile Computing and Networking, ACM*, 2000; 56–67.
30. Braginsky D, Estrin D. Rumor routing algorithm for sensor networks. In *Proceedings of the 1st ACM International Workshop on Wireless Sensor Networks and Applications, ACM*, 2002; 22–31.
31. Lou W. An efficient N-to-1 multipath routing protocol in wireless sensor networks. In *IEEE International Conference on Mobile Ad Hoc and Sensor Systems Conference 2005, IEEE*, 2005; 8–672.
32. Du X, Lin F. Improving routing in sensor networks with heterogeneous sensor nodes. In *Vehicular Technology Conference 2005 (VTC 2005)—Spring 2005 IEEE 61st*, Vol. 4. IEEE, 2005; 2528–2532.
33. Akkaya K, Younis M. A survey on routing protocols for wireless sensor networks. *Ad Hoc Networks* 2005; **3**(3): 325–349.
34. Teng J, Snoussi H, Richard C. Binary variational filtering for target tracking in sensor networks. *IEEE Workshop on Statistical Signal Processing* Aug. 2007: 685–689.
35. Vermaak J, Lawrence N, Perez P. Variational inference for visual tracking. In *2003 IEEE Computer Society Conference on Computer Vision and Pattern Recognition, 2003. Proceedings*, Vol. 1, 2003.
36. Snoussi H, Richard C. Ensemble learning online filtering in wireless sensor networks. In *10th IEEE Singapore International Conference on Communication systems 2006 (ICCS 2006)*, 2006; 1–5.
37. Yang H, Sikdar B. A protocol for tracking mobile targets using sensor networks. In *Proceedings of the First IEEE International Workshop on Sensor Network Protocols and Applications 2003*, 2003; 71–81.
38. Cui S, Goldsmith A, Bahai A. Energy-constrained modulation optimization. *IEEE Transactions on Wireless Communications* 2005; **4**(5): 2349–2360.
39. Ikki S, Ahmed M. Performance analysis of cooperative diversity wireless networks over Nakagami-m fading channel. *IEEE Communications Letters* 2007; **11**(4): 334.
40. Valenzuela R. A statistical model for indoor multipath propagation. *IEEE Journal on Selected Areas in Communications* 1987; **5**(2): 128–137.
41. Simon M, Alouini M. *Digital Communication Over Fading Channels*. Wiley-IEEE Press: New York, 2005.
42. Papoulis A, Pillai S. *Probability, Random Variables and Stochastic Processes*. McGraw-Hill Education (India) Pvt Ltd, 2002.
43. Zuo L, Niu R, Varshney P. A sensor selection approach for target tracking in sensor networks with quantized measurements. In *Proceedings of the 2007 IEEE International Conference on Acoustics, Speech, and Signal Processing, II*; 2521 –2524.
44. Heinzelman W, Chandrakasan A, Balakrishnan H. Energy-efficient communication protocol for wireless microsensor networks. In *Proceedings of the 33rd Hawaii International Conference on System Sciences*,

Vol. 8. IEEE Computer Society: Washington, DC, USA, 2000; 8020.

AUTHOR'S BIOGRAPHY

Majdi Mansouri was born 11 November 1982 in Kasserine, Tunisia. He received the Diplom-Ingenieur degree in 2006 from High School of Communications of Tunis (SUP'COM) and the MS degree in 2008 from High school of Electronic, Informatique and Radiocommunications in Bordeauxx (ENSEIRB). He received the PhD degrees in 2011 from Troyes University of Technology, France. He is currently a postdoctoral research associate at Texas A&M University at Qatar. His current research interests include statistical signal processing and wireless sensors networks. Mansouri is the author of over 25 papers.